Rapid Communications

Analysis of over-magnetization of elemental transition metal solids from the SCAN density functional

Daniel Mejía-Rodríguez* and S. B. Trickey†
Quantum Theory Project, Department of Physics, University of Florida, Gainesville, Florida 32611, USA

(Received 5 April 2019; revised manuscript received 21 June 2019; published 18 July 2019)

Recent investigations have found that the strongly constrained and appropriately normed (SCAN) meta-generalized gradient approximation exchange-correlation functional significantly over-magnetizes elemental Fe, Co, and Ni solids. For the paradigmatic case, bcc Fe, the error relative to experiment is $\gtrsim$20%. A comparative analysis of magnetization results from SCAN and its *deorbitalized* counterpart, SCAN-L, leads to identification of the source of the discrepancy. It is not from the difference between Kohn-Sham (SCAN-L) and generalized Kohn-Sham (SCAN) procedures. The key is the iso-orbital indicator α (the ratio of the local Pauli and Thomas-Fermi kinetic energy densities). Its *deorbitalized* counterpart α_L has more dispersion in both spin channels with respect to magnetization in an approximate region between 0.6 and 1.2 bohrs around an Fe nucleus. The overall effect is that the SCAN switching function evaluated with α_L reduces the energetic disadvantage of the down channel with respect to up compared to the original α, which in turn reduces the magnetization. This identifies the cause of the SCAN magnetization error as insensitivity of the SCAN switching function to α values in the approximate range $0.5 \lesssim \alpha \lesssim 0.8$ and oversensitivity for $\alpha \gtrsim 0.8$.

DOI: 10.1103/PhysRevB.100.041113

Transition metals generally—and Fe particularly—are central to both practical applications and to the development of improved exchange-correlation (XC) approximations for use in density functional calculations. A pertinent example of the latter role is the generalized gradient approximation (GGA) [1,2] breakthrough that gave the right ground-state crystal structure and magnetic order for elemental Fe [3]. In light of that importance, some results from a very sophisticated meta-GGA functional are quite provocative.

Several authors have found that the strongly constrained and appropriately normed (SCAN) [4,5] meta-GGA XC functional over-magnetizes some elemental transition metals [6–11]. For example, Isaacs and Wolverton [6] found that SCAN over-magnetizes bcc Fe by 19%, hcp Co by 8%, and fcc Ni by 14%. They also found that "...[based on local moment calculations] the average maximum magnetic moment within SCAN is 12% larger than that found within PBE." Data from Jana *et al.* [7] correspond to magnetization excesses of 20% (bcc Fe), 4% (fcc Co), and 8% (fcc Ni). In the ferromagnetic Fe_3Pt alloy, Romero and Verstraete [8] found that SCAN gave ≈15% over-magnetization on the Fe site compared to 3% overage from the Perdew-Burke-Ernzerhof (PBE) functional. Ekholm *et al.* [9] found excesses of 25% for bcc Fe, 9.5% for hcp Co, and 28% for fcc Ni.

Most recently, Fu and Singh [10] showed that SCAN over-magnetizes bcc Fe by ≈23%, hcp Co by 14%, and fcc Ni by 13%. In Fe_3C, they found SCAN gives nearly 30% over-magnetization per three-iron-atom formula unit. Subsequently they [11] have suggested that the SCAN functional is intermediate between PBE and approaches that describe more localized systems better [e.g., hybrid functionals or density functional theory with Hubbard U (DFT+U)], hence SCAN tends to yield over-magnetization.

Overall, the trend is completely clear. SCAN over-magnetizes elemental transition metal solids. Presumably the numerical differences (compared for the same crystalline phases) trace to differences in computational parameters and techniques and to the intrinsic sensitivity of magnetization calculations. Given the other broad successes of SCAN (e.g., Ref. [6] and references therein), the discrepancy is noteworthy. SCAN results for these simple systems are strikingly different from the behavior found from other meta-GGA functionals [e.g., Tao-Perdew-Staroverov-Scuseria (TPSS) [12]] or a typical GGA (e.g., PBE [13]). Both give close to the experimental magnetization.

The unresolved issue is the specific source of the discrepancy: What within the SCAN functional leads to such strikingly different magnetization behavior compared to other semilocal functionals? With the aid of SCAN-L [14,15], our *deorbitalized* version of SCAN, we can resolve the issue and, as well, provide insight perhaps useful for the development of better meta-GGA functionals.

A few definitions are useful. SCAN uses the so-called iso-orbital indicator

$$\alpha(\mathbf{r}) := (\tau_s - \tau_W)/\tau_{\mathrm{TF}}. \tag{1}$$

Here, $\tau_s = (1/2)\sum f_j |\nabla \varphi_j(\mathbf{r})|^2$ is the positive-definite Kohn-Sham (KS) kinetic energy density in terms of the KS orbitals φ_j (with occupations f_j), and τ_W and τ_{TF} are the von Weizsäcker and Thomas-Fermi kinetic energy densities, respectively. The numerator of α is the Pauli kinetic energy (KE) density. It vanishes for the case of a single-orbital

*dmejiarodriguez@ufl.edu
†trickey@qtp.ufl.edu

TABLE I. Calculated bcc Fe lattice parameters, saturation magnetizations, and FSM energies for various XC functionals at a_{calc}.

	a_{calc} (Å)	m_{sp} (μ_B/atom)	E_{mag} (meV/atom)
PBE	2.82	2.14	−564
TPSS	2.80	2.12	−645
SCAN	2.85	2.60	−1100
regSCAN	2.84	2.62	−1201
SCAN-L	2.81	2.05	−653
TPSS-L	2.81	2.09	−568

system, one of the ways that α enables a functional to distinguish chemically different bonding regions. The deorbitalized SCAN, SCAN-L, differs only in using an approximate orbital-independent $\alpha[n, \nabla n, \nabla^2 n]$ with n the electron number density.

Turning to analysis, first we can eliminate the possibility that the SCAN magnetization discrepancies arise from limitations of computational technique. The potential issue is that projector augmented-wave (PAW) data sets do not exist for SCAN (nor for other meta-GGAs). Thus the VASP calculations [16,17] reported here and earlier [6,9–11] used PBE PAWs instead. However, in addition to those calculations, two groups [9–11] also did post-self-consistent field (SCF) all-electron calculations with the WIEN2K code [18] and PBE spin densities and found the same distinctive over-magnetization trend for SCAN.

Therefore the issue originates structurally in SCAN. An obvious question is whether SCAN-L, which uses the same structure as SCAN, inherits the over-magnetization. Table I shows results of VASP [16] calculations (with PAWs [17] and other parameters as in Ref. [15]). SCAN and SCAN-L yield qualitatively different magnetizations. Consistent with prior results summarized above, in our fixed spin-moment (FSM) calculations SCAN gives an overly stable bcc Fe structure that is over-magnetized: $m_{sp} = 2.60\mu_B$ at FSM energy $|E_{\text{mag}}| =$ 1100 meV below zero moment at the calculated equilibrium lattice parameter. For comparison, the PBE values are $2.21\mu_B$ and 564 meV.

Figure 1 (the counterpart to Fig. 1 of Ref. [10]) shows the dramatic difference in FSM energy as a function of magnetization for SCAN compared to other functionals. In contrast to the SCAN magnetization, SCAN-L reduces both $|E_{\text{mag}}|$ and m_{sp} to the point of being essentially the same as the PBE results. (Aside: The kinked behavior of the SCAN $|E_{\text{mag}}|$ at $m \approx 0.3\mu_B$ seems to arise from numerical instabilities. It does not appear in the post-SCF SCAN curve in Fig. 1 of Ref. [10] and is immaterial to the issue at hand.)

Upon first thought, the origin of the difference between SCAN and SCAN-L magnetization might be suspected to have arisen from the procedural difference associated with use of orbital-dependent and orbital-independent functionals. The orbital independence of SCAN-L leads to a multiplicative XC potential and use of the ordinary Kohn-Sham (KS) procedure. The orbital-dependent SCAN XC potential, in contrast, almost always is used in the generalized Kohn-Sham (gKS) context. The two schemes are inequivalent [19]. However, $m_{sp}(a_{\text{calc}})$ values for bcc Fe from the TPSS functional [12], obtained with gKS, and from its deorbitalized version,

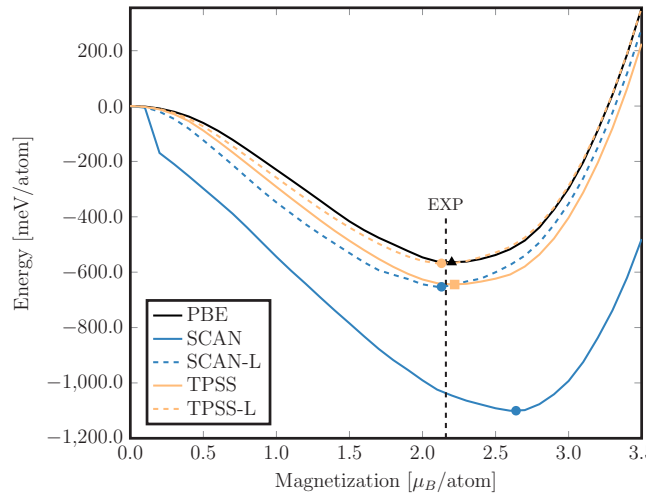

FIG. 1. Fixed spin-moment energy vs magnetic moment for bcc Fe at a_{exp} from PBE, SCAN, SCAN-L, TPSS, and TPSS-L. Dots show minimum FSM energy values. Experimental value from Ref. [10].

TPSS-L, which uses KS, do not exhibit the remarkable difference of the SCAN vs SCAN-L case. TPSS and TPSS-L deliver m_{sp} values indistinguishable from each other and from the PBE result (see Fig. 1).

The post-SCF calculations quoted already [9–11] in fact confirm the irrelevance of KS and gKS for over-magnetization. The sole difference between the post-SCF SCAN energy and the underlying PBE energy is the exchange-correlation energy E_{xc} evaluation. The two calculations differ only by $E_{\text{xc}}^{\text{SCAN}}[\{\phi_j^{\text{PBE}}\}] - E_{\text{xc}}^{\text{PBE}}[n_{\text{PBE}}]$. They are evaluated

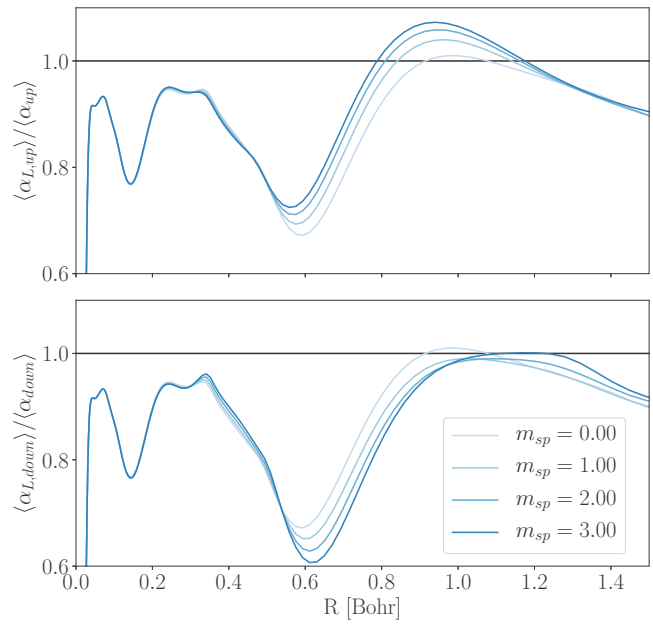

FIG. 2. Ratio of angularly averaged α's, $\langle\alpha_L\rangle/\langle\alpha\rangle$ for spin-up (above) and spin-down (below) as function of radial distance from Fe nucleus (evaluated with bcc Fe PBE densities) at selected fixed spin moments.

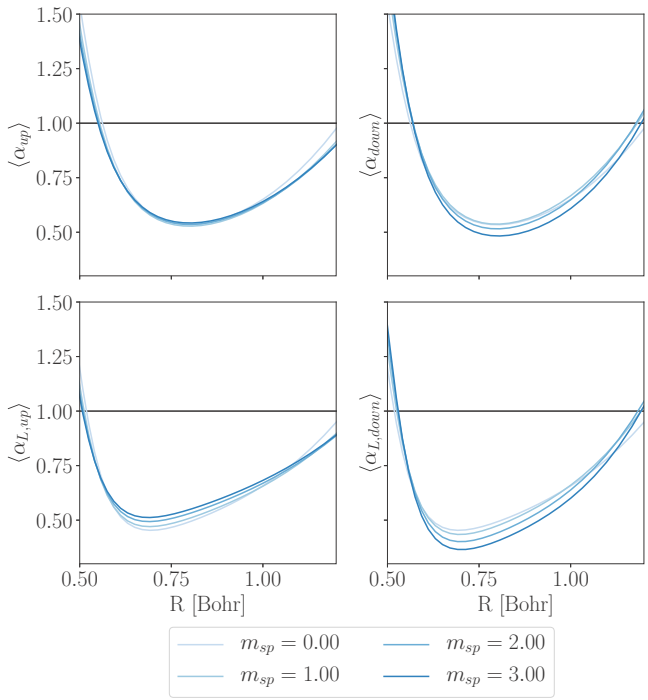

FIG. 3. Angularly averaged α (above) and α_L (below) as a function of radial distance from a Fe nucleus (evaluated with bcc Fe PBE densities) at selected fixed spin moments. Spin-up plots are in the left column, spin-down in the right.

entirely with KS quantities. There are no gKS inputs. Nevertheless, in the post-SCF calculations SCAN over-magnetizes. In this context, it also is worth mentioning that those post-SCF results are incompatible with the localization explanation offered in Ref. [11], since PBE calculations suffer from delocalization error due to self-interaction. (The extent, if any, to which SCAN causes localization to occur in the self-consistent VASP calculations reported here and earlier is indeterminate at this point. That follows from the inherent spurious delocalization in the PBE PAWs used. The issue is irrelevant to the analysis below.)

The only other difference between SCAN and SCAN-L is the distinction between α and α_L. In most cases, $\alpha_L \approx \alpha$ is very accurate, but there can be regions where their difference is noticeable [14,20]. That is critical to the present analysis. Figure 2 shows the ratio of the angularly averaged α_L to α for various magnetizations as a function of distance from the Fe nucleus in bcc Fe (calculated post-SCF with bcc Fe spin densities from PBE).

Key distinctions to note include the fact that below about $r = 0.9$ bohrs, α_L is smaller than α for both spins, with particularly strong reduction on $0.6 \lesssim r \lesssim 0.8$ bohrs. It also is important that the ratios for both spins exhibit some dispersion with respect to m_{sp}, especially in the same $0.6 \lesssim r \lesssim 0.8$ bohrs region. Figure 3 shows that such dispersion is present in both spin channels of α_L, but only in the spin-down channel of α. Moreover, $\alpha_{L,\text{down}}$ is more dispersed than α_{down}.

The dominant α-dependent contribution to exchange in SCAN and SCAN-L is from the switching function $f_x(\alpha)$ that distinguishes regions of $\alpha < 1$ and $\alpha > 1$.

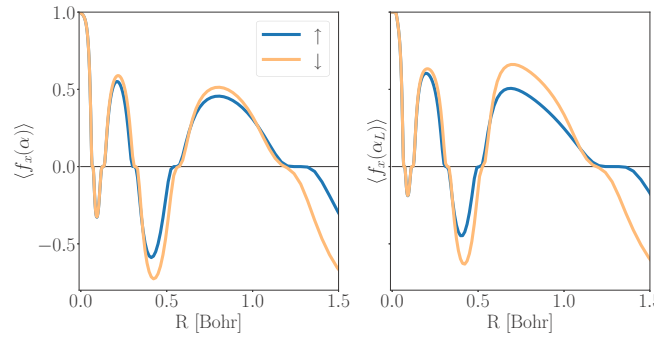

FIG. 4. Left: Angularly averaged SCAN switching function $f_x(\alpha)$ as a function of radial distance from the Fe nucleus (evaluated with bcc Fe PBE spin densities) at $m_{sp} = 2.5\mu_B$/atom. Right: Radial behavior of the angularly averaged SCAN switching function evaluated with α_L, $f_x(\alpha_L)$, for the same densities.

An important bit of analysis is that recently it has been shown [21] that modifications to make f_x smoother around $\alpha \approx 1$ have a negligible effect on SCAN structural and energetic predictions in solids. Our calculations with that "regularized SCAN" (regSCAN) confirm similarly little effect of those modifications upon the over-magnetization values of m_{sp} and a 9% increase on $|E_{\text{mag}}|$ (see Table I).

Figure 4 shows the angularly averaged switching function as a function of radial distance evaluated with α and α_L for both spin channels. One sees that on $0.6 \lesssim r \lesssim 0.9$ bohrs or so, the α_L values separate the up- and down-spin points on the $f_x(\alpha)$ curve more than the original α does. In particular, because the down-spin ratio α_L to α is below the up-spin ratio in that radial domain, the down-spin exchange energy density $e_{x,\text{down}}$ contributes more to the full e_x for SCAN-L than for SCAN. The dispersion ordering with respect to magnetization of $\alpha_{L,\text{up}}$ values is reversed compared to $\alpha_{L,\text{down}}$. That is, for up spin, the greatest magnetization has the least reduction (largest $\langle\alpha_{L,\text{up}}\rangle/\langle\alpha_{\text{up}}\rangle$) while for down spin, the greatest magnetization has the greatest reduction (least $\langle\alpha_{L,\text{down}}\rangle/\langle\alpha_{\text{down}}\rangle$). Added to this is the fact that the up-spin α is almost insensitive to m_{sp}, hence so is the up-spin e_x, which is not the case for α_L.

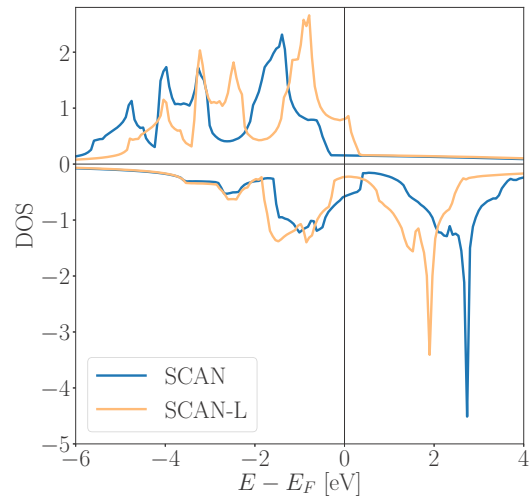

FIG. 5. bcc Fe densities of states for SCAN and SCAN-L. Up spin, upper panel; down spin, lower panel.

TABLE II. Co, Ni and V calculated saturation magnetizations and FSM energies for various XC functionals at a_{exp}.

	m_{sp} (μ_B/atom)	E_{mag} (meV/atom)
hcp Co		
PBE	1.65	−255
SCAN	1.80	−578
SCAN-L	1.63	−277
fcc Ni		
PBE	0.65	−60
SCAN	0.78	−137
SCAN-L	0.67	−74
bcc V		
PBE	0.00	0
SCAN	0.57	−6
SCAN-L	0.00	0

In the immediately adjacent region, $0.9 \lesssim r \lesssim 1.2$ bohrs, $\alpha_{\text{down}} > \alpha_{\text{up}}$ and $\alpha_{L,\text{down}} > \alpha_{L,\text{up}}$. However, the α_L's are closer together. As a result, $e_{x,\text{down}}$ also contributes more to the full e_x for SCAN-L than for SCAN in this region.

The net result is a set of significant differences in the densities of states of the ground states predicted by SCAN and SCAN-L. Figure 5 shows that, relative to SCAN, SCAN-L shifts the up-spin occupied states up somewhat, thereby reducing the magnetization energy and leaving their population reduced. Meanwhile, the down-spin state energies are somewhat lowered, corresponding to enhanced $e_{x,\text{down}}$ and their population therefore goes up. Those shifts may also be related to the increased exchange splittings discussed in Ref. [11].

Since discrepancies of α_L with respect to α identify the region $0.6 \lesssim r \lesssim 1.2$ bohrs as critical, we tried a simple modification of the SCAN switching function solely to probe how it responds to the actual orbital-dependent α values in that region. The deorbitalized α_L values for up and down spin are more separated than the original α's in the $0.6 \lesssim r \lesssim 0.9$ bohrs region (region A), but closer together in the $0.9 \lesssim r \lesssim 1.2$ bohrs one (region B). Another important fact is that α and α_L values in both such regions are below 1, but get closer to 1 in region B. An important probe therefore is to bring the values of the switching function for α_{up} closer to the ones for α_{down} in region B, while separating the switching function values in region A. This amounts to investigating the consequences of reducing the sensitivity of the switching function to small changes in its argument around $0.8 \lesssim \alpha \leqslant 1$ and increasing that sensitivity for $\alpha \lesssim 0.8$.

For $\alpha < 1$ [see Eqs. (58)–(60) in Ref. [15]], the switching function is $f_x(\alpha) = \exp[-c_{1x}\alpha/(1-\alpha)]$ with $c_{1x} = 0.667$. A crude way to probe the apparently desirable sensitivity change for region B is to increase c_{1x} from 0.667 to 1. Doing so yields improved m_{sp} and E_{mag} values for bcc Fe, but produces mixed results for other systems. Detailed pursuit of more sophisticated modifications would be tantamount to constructing a revision or successor to SCAN, a task far beyond the scope of the present investigation.

What the simple probe and the comparative analysis of α and α_L behavior make clear is the significant need for more refined switching functions in improved meta-GGA functionals. In addition to the over-magnetization origin diagnosed here, the SCAN switching function can be linked to issues of numerical integration sensitivity [19] and self-consistent field stability [21]. To that point, it is perhaps suggestive that the Tao and Mo meta-GGA XC functional [22], which uses a very different switching function, does not give over-magnetization [7].

For completeness, Table II shows the calculated saturation magnetization and FSM energies for hcp Co, fcc Ni, and bcc V. For Co, SCAN-L reduces m_{sp} relative to SCAN by about 9%. For Ni the SCAN-L reduction is 14%. The vanadium case is particularly notable, because SCAN wrongly predicts a magnetic ground state, whereas PBE and SCAN-L have nonmagnetic ground states.

In summary, we have found that the SCAN over-magnetization arises from subtle differences in the behavior of the iso-orbital indicator α for each spin channel that are magnified by the SCAN switching function, especially for $\alpha < 1$. In contrast, the approximate nature of the orbital-independent α_L offsets those magnifications in a remarkably precise but serendipitous way. Two approaches for the development of new meta-GGA functionals are suggested by this analysis. One would be to devise switching functions which are better adapted to the physics signaled by the iso-orbital indicator α. The other would be to use a different iso-orbital indicator [23] that behaves more like the approximate α_L in the cases considered. One other possible consideration is that SCAN parameter values are determined, among other constraints, by appropriate norms. None of them is a spin-polarized case. As a consequence, SCAN relies solely on the spin-scaling relations for its magnetization predictions. A new or augmented set of norms might be useful.

We thank Fabien Tran for a helpful remark about WIEN2K and David Singh for an informative discussion. This work was supported by U.S. Department of Energy Grant No. DE-SC 0002139. S.B.T. also was supported by U.S. Department of Energy Energy Frontier Research Center Grant No. DE-SC 0019330.

[1] J. P. Perdew, in *Electronic Structure of Solids '91*, edited by P. Ziesche and H. Eschrig (Akademie, Berlin 1991), p. 11.

[2] J. P. Perdew, J. A. Chevary, S. H. Vosko, K. A. Jackson, M. R. Pederson, D. J. Singh, and C. Fiolhais, Phys. Rev. B **46**, 6671 (1992).

[3] D. J. Singh, W. E. Pickett, and H. Krakauer, Phys. Rev. B **43**, 11628 (1991).

[4] J. Sun, A. Ruzsinszky, and J. P. Perdew, Phys. Rev. Lett. **115**, 036402 (2015).

[5] J. Sun, R. C. Remsing, Y. Zhang, Z. Sun, A. Ruzsinszky, H. Peng, Z. Yang, A. Paul, U. Waghmare, X. Wu, M. L. Klein, and J. P. Perdew, Nat. Chem. **8**, 831 (2016).

[6] E. B. Isaacs and C. Wolverton, Phys. Rev. Mater. **2**, 063801 (2018).

[7] S. Jana, A. Patra, and P. Samal, J. Chem. Phys. **149**, 044120 (2018)
[8] A. H. Romero and M. J. Verstraete, Eur. Phys. J. B **91**, 193 (2018).
[9] M. Ekholm, D. Gambino, H. J. M. Jönsson, F. Tasnádi, B. Alling, and I. A. Abrikosov, Phys. Rev. B **98**, 094413 (2018).
[10] Y. Fu and D. J. Singh, Phys. Rev. Lett. **121**, 207201 (2018).
[11] Y. Fu and D. J. Singh, Phys. Rev. B **100**, 045126 (2019).
[12] J. Tao, J. P. Perdew, V. N. Staroverov, and G. E. Scuseria, Phys. Rev. Lett. **91**, 146401 (2003).
[13] J. P. Perdew, K. Burke, and M. Ernzerhof, Phys. Rev. Lett. **77**, 3865 (1996).
[14] D. Mejía-Rodríguez and S. B. Trickey, Phys. Rev. A **96**, 052512 (2017).
[15] D. Mejía-Rodríguez and S. B. Trickey, Phys. Rev. B **98**, 115161 (2018).
[16] G. Kresse and J. Furthmüller, Phys. Rev. B **54**, 11169 (1996).
[17] G. Kresse and D. Joubert, Phys. Rev. B **59**, 1758 (1999).
[18] P. Blaha, K. Schwarz, G. K. H. Madsen, D. Kvasnicka, and J. Luitz, *WIEN2k, An Augmented Plane Wave + Local Orbitals Program for Calculating Crystal Properties* (Vienna University of Technology, Vienna, 2001).
[19] Z.-H. Yang, H. Peng, J. Sun, and J. P. Perdew, Phys. Rev. B **93**, 205205 (2016).
[20] F. Tran, P. Kovacs, L. Kalantari, G. K. H. Madsen, and P. Blaha, J. Chem. Phys. **149**, 144105 (2018).
[21] A. P. Bartók and J. R. Yates, J. Chem. Phys. **150**, 161101 (2019).
[22] J. Tao and Y. Mo, Phys. Rev. Lett. **117**, 073001 (2016).
[23] J. W. Furness and J. Sun, Phys. Rev. B **99**, 041119(R) (2019).